CHEMISTRY
A EUROPEAN JOURNAL

DOI: 10.1002/chem.200501010

Selective Heterogeneous Nucleation and Growth of Size-Controlled Metal Nanoparticles on Carbon Nanotubes in Solution

Yu Wang,[a] Xin Xu,*[a] Zhongqun Tian,[a] Ye Zong,[a] Huiming Cheng,[b] and Changjian Lin*[a]

Abstract: We present a novel approach to the in situ deposition of size-controlled platinum nanoparticles on the exterior walls of carbon nanotubes (CNTs). The reduction of metal ions in ethylene glycol (EG), by the addition of a salt such as sodium dodecyl sulfate (SDS), *p*-$CH_3C_6H_4SO_3Na$, $LiCF_3SO_3$, or $LiClO_4$, results in high dispersions and high loadings of platinum nanoparticles on CNTs without aggregation. We have performed controlled experiments to elucidate the mechanism. By exploiting the salt effect, our method effectively depresses homogeneous nucleation, leading to selective heterogeneous metal nucleation and growth, even on unmodified CNTs. In the 2.3–9.6 nm size range, the size of platinum nanoparticles, at 50% loading, can be controlled by changing the concentration of metal ions, the reaction temperature, the reducing reagent or the means by which reactive solutions are added. Our method provides a flexible route towards the preparation of novel one-dimensional hybrid materials, for which a number of promising applications in a variety of fields can be envisioned.

Keywords: carbon · nanotubes · platinum · salt effect

Introduction

Metal/carbon-nanotube (metal/CNT) hybrid materials are of considerable interest for their application in the area of nanoelectronics, as biosensors, in heterogeneous catalysis and in electrocatalysis.[1] The controlled coating of metal nanoparticles onto CNTs and the prevention of aggregation of these particles are of primary importance for the successful application of these materials. So far, several methods have been developed to coat or deposit metals onto CNTs. These methods include impregnation,[1d,2–4] electroless plating,[5] self-assembly,[6] electrodeposition,[7] and physical vapor deposition.[1b,8]Impregnation is the most widely used wet-chemical method.[1d–f,2–4,9–11] This method is generally very simple to implement and is thus an attractive choice for large-scale synthesis. However, the bottleneck for the impregnation method lies in the competition between homogeneous nucleation and heterogeneous nucleation; this leads to aggregation of the metal nanoparticles in solution instead of the selective deposition of metals on the supports.[1f,9,10,11c] When using DNA as a biomolecular support, metal-coated DNA can be readily obtained upon reduction of a solution containing both DNA and a metal salt, since DNA strands offer a variety of binding sites for metal ions.[11] Carefully designed experiments have demonstrated that selective heterogeneous metallization can only be achieved if the metal ions are covalently bound to the DNA bases before reduction.[11] The realization of selective metal deposition on CNT supports presents a greater challenge, since the pristine surfaces of CNTs are inert.[12] To overcome this difficulty, one could either decrease the activation barrier towards heterogeneous nucleation, or alternatively increase that towards homogeneous nucleation. To date, efforts have focused mainly on the former, with limited success.[2–5] Carboxylic acid functional groups, for instance, can be introduced onto the surfaces of CNTs by means of chemical treatment under harsh acidic conditions. These functional groups not only enhance the solubility of the CNTs, but coordination of

[a] Dr. Y. Wang, Prof. Dr. X. Xu, Prof. Dr. Z. Tian, Y. Zong, Prof. Dr. C. Lin
State Key Laboratory for Physical Chemistry of Solid Surfaces and College of Chemistry and Chemical Engineering Xiamen University
361005 Xiamen (China)
Fax: (+86) 218-3047
E-mail: xinxu@xmu.edu.cn
cjlin@xmu.edu.cn

[b] Prof. Dr. H. Cheng
Institute of Metal Research
Chinese Academy of Sciences
110015 Shenyang (China)

Supporting information for this article is available on the WWW under http://www.chemeurj.org/ or from the author.

these groups to the metal ions also gives rise to preferred sites of nucleation.[2–3] In the process of electroless plating, catalytic seeds have to be introduced in order to activate the strong-acid-treated tubes and hence to achieve a better decoration.[5] In addition to aqueous or organic solutions, supercritical CO_2 and water have also been employed as reaction media.[4] Supercritical fluids are characterized by low viscosity, high diffusivity, near-zero surface tension, and strong solvent power. These properties facilitate the delivery of reactants to small holes or to narrow tubes, leading to an improved decoration of metals on CNTs.[4] Despite these studies, selective deposition of highly dispersed metal nanoparticles on CNTs by the wet-chemical method, with size and loading control, has not yet been reported.

In the self-assembly method, the metal nanoparticles are synthesized and then subsequently attached to the surfaces of the nanotubes through the non-covalent interactions of link molecules.[6] This approach may avert the competition between the homogeneous and heterogeneous nucleation of the metal. The main advantage of the self-assembly method is that it can realize selective coating of nanoparticles on CNTs. Although self-assembly is a promising method, the presence of the organic protecting shell may or may not hinder the catalytic function of metal nanoparticles.[13] Indeed, the organic protecting shell will certainly degrade such properties as electric conductivity, which, in turn, will impair electrocatalytic performance. Besides, self-assembly is a tedious and expensive method, and therefore unsuitable for large-scale synthesis.

Pt and Pt-based nanoparticles are of considerable interest for application in low-temperature fuel cells. To disperse precious metals and to improve their catalytic efficiency, it is common to use high-surface-area carbons as supports. Difficulties in achieving high dispersion and high loading on active carbon and CNTs have led to the development of alternative carbon supports using novel nanostructures. Recently, mesoporous carbon members,[9a,b] carbon nanocoils,[9c] and cup-stacked-type carbon nanofibers[9d] have been synthesized and used as catalyst supports. Highly dispersed Pt or Pt-Ru nanoparticles supported on these carbon nanomaterials, with high loading, can be prepared by the impregnation method, and these materials show enhanced electrocatalytic performance.[9]

In this work we demonstrate a novel synthetic route towards selective heterogeneous metal nucleation and growth on modified and unmodified CNTs. This is realized by adding some salts to the reaction system, which efficiently increase the barrier towards homogeneous metal nucleation. We report the results for Pt, a metal of high technological importance.[1e,f,9] The size of Pt nanoparticles on CNTs can be easily controlled by our method, which offers a promising pathway to preparing supported metal nanoparticles of high dispersion and/or of high loading.

Results and Discussion

Preparation of Pt-coated CNTs: The morphology of the typical product was investigated by means of transmission electron microscopy (TEM) (Figure 1 and Figure S1 in the Supporting Information). From Figure 1A,B, it is clear that the CNTs were coated with a dense layer of Pt nanoparticles (Pt loading = 50 wt %). Most importantly, aggregation of metal particles in solution was not observed, indicating that homogeneous nucleation was depressed. The high-resolution TEM (HRTEM) images shown in Figure 1B show the interface between Pt nanoparticles and the surfaces of multiple-walled nanotubes (MWNTs). Instead of being perfectly spherical, the Pt nanoparticles were flat on the bottom, thus ensuring a large contact surface with the CNTs. This is a strong indication that the particles were formed by heterogeneous nucleation on the CNT surface, with subsequent

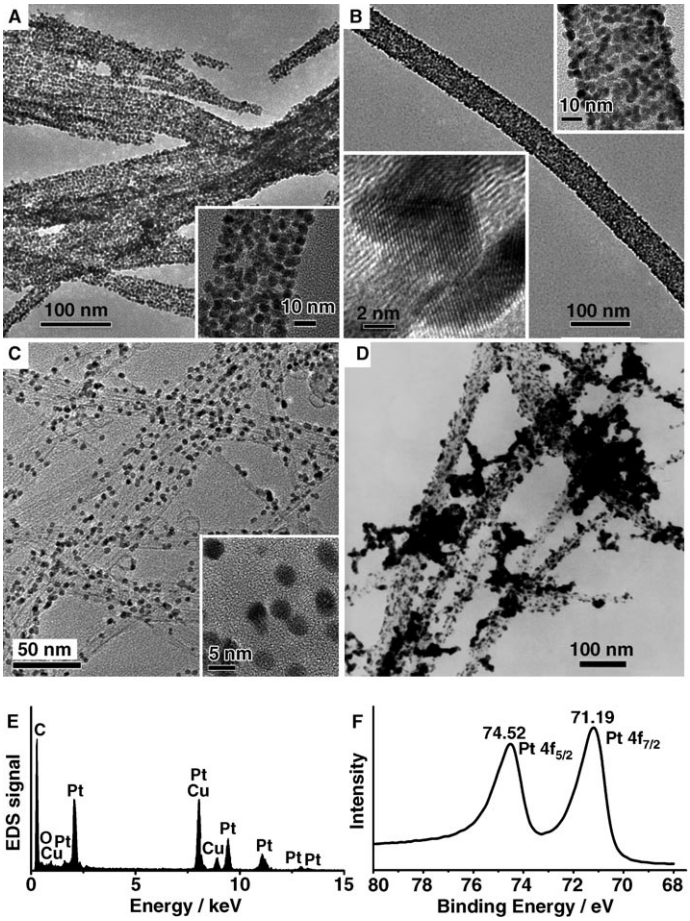

Figure 1. TEM images for Pt-coated CNTs. The insets show the corresponding high magnification TEM images (A–C): A) Pt-coated SWNTs (50 wt %); B) Pt-coated MWNTs (50 wt %); C) Pt-coated SWNTs (10 wt %). D) Pt-coated SWNT samples prepared in the absence of SDS. E) The EDS analysis for Pt-coated SWNTs (50 wt %). F) Pt-4f fine structure from XPS spectra for Pt-coated SWNTs. More details are provided in Figure S1 in the Supporting Information.

growth of these nuclei then resulting in a nanoparticle coating on the CNTs.

The presence of Pt in the as-prepared Pt-coated single-walled nanotubes (SWNTs) was confirmed by X-ray energy-dispersive spectroscopy (EDS) (Figure 1E) and X-ray photoelectron spectroscopy (XPS; Figure S1 in the Supporting Information). No other heteroelement such as Cl or S was detected. The 4f fine structure obtained by XPS (Figure 1F) shows that the peak binding energy for Pt $4f_{7/2}$ is at 71.19 eV and that for Pt $4f_{5/2}$ is at 74.52 eV. The measured full width at half maximum (FWHM) for Pt $4f_{7/2}$ is 1.15 eV (pass energy 29.35 eV), which can be compared with the standard for Pt $4f_{7/2}$ (pass energy 23.5 eV; FWHM 1.03 eV). All of the above evidence indicates that Pt in the as-prepared Pt-coated SWNTs exists in the pure metallic state. In comparison with the incipient-wetness impregnation method, in which the metallic-Pt deposit on CNTs is obtained by calcination in air (to decompose the precursor) and subsequent reduction in H_2, our method is more effective for the selective deposition of metal nanoparticles on CNTs, and moreover, the purity of Pt is also higher.[2g]

Figure 1C shows the TEM image of Pt-coated CNTs with a nominal Pt loading of 10 wt%, wherein Pt nanoparticles of about 3 nm are dispersed uniformly on the exterior surfaces of the CNTs. Our method is thus applicable to the fabrication of both densely Pt-coated CNTs (important as metallic nanowires in nanodevices; Figure 1A,B)[1b] and highly dispersed Pt-coated CNTs (important as heterogeneous catalysts; Figure 1C).[9–10]

It is widely believed that selective heterogeneous metal growth on CNTs can only be achieved by the creation of preferential nucleation sites on CNTs through chemical modification.[2–3] However, chemical modification of CNTs under harsh acidic conditions may break the symmetry of the π-bonding arising from sp^2 hybridization, and thereby deteriorate their unique electronic properties, which are so important for their application as nanodevices.[14] We show here that chemical modification of CNTs is not a prerequisite in our method. Thus selective metal deposition can be achieved in equally efficiently for SWNTs with pretreatment (Figure 1A) and MWNTs without pretreatment (Figure 1B).

Significantly, we found that sodium dodecyl sulfate (SDS) plays a critical role in directing heterogeneous nucleation and growth. In the absence of SDS, a similar experiment resulted in only a small amount of deposition of Pt nanoparticles on CNTs; a very large part of the Pt dissociated from the CNTs and formed aggregates in solution (Figure 1D). This is in sharp contrast to the results obtained in the presence of SDS as shown in Figure 1A–C.

Mechanism for selective heterogeneous nucleation and growth: We examined how SDS would affect the homogeneous nucleation of Pt in solution. Heating of solutions of H_2PtCl_6 (0.25 mg mL^{-1}) in ethylene glycol (EG), both with and without SDS (2%), at a rate of 1 °C min^{-1} caused the original pale yellow solution to discolor at around 127 °C, indicating that Pt ions were reduced in solution. As the temperature of the solution approached 137 °C, the solution without SDS started to show instability either by depositing a Pt mirror on the flask wall or by forming dark Pt precipitates. In contrast, the solution containing SDS was considerably more stable, remaining colorless and clear for more than 30 min even at 137 °C. When SWNTs (1 mg) were then dispersed in the latter solution, a large amount of Pt was deposited on the SWNTs, as evidenced by the TEM images (Figure S2 in the Supporting Information).

We claim that, for solutions of H_2PtCl_6 (0.25 mg mL^{-1}) in EG, with or without SDS, 138 °C is a critical temperature, above which darker Pt precipitates formed rapidly in solutions. However, TEM images reveal that in the solution without SDS, Pt formed a floc (an aggregate having a rather loose and open structure; Figure 2A), whereas in the solution containing SDS, Pt formed a coagulum (an aggregate with a dense structure) of size 100–200 nm (Figure 2B). HRTEM images show that both the coagulum and floc are composed of small metal particles. X-ray diffraction (XRD)

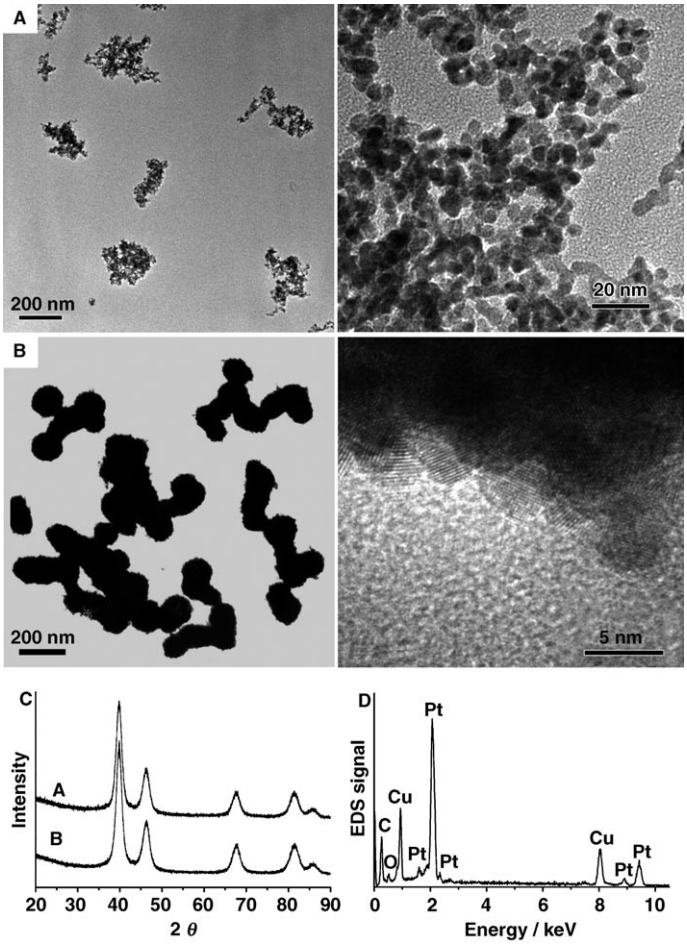

Figure 2. Homogeneous aggregation of Pt nanoparticles in solutions in the absence of CNTs. TEM images of samples prepared without SDS (A) and with SDS (B). The right-hand images are enlargements of sections of the left-hand images. More details are provided in Figure S3 in the Supporting Information.

analyses reveal a crystallite size of 4.6 nm in both Pt floc and Pt coagulum (Figure 2C).

Sample TEM images (Figure S3 in the Supporting Information) demonstrate how the process of aggregation evolved as a function of time. In the presence of SDS, the newly formed Pt nanoparticles agglomerated within about 2 min to form a stable coagulum (Figure S3 in the Supporting Information). As coagulation did not occur in the solution without SDS, we infer that the surface energy of the newly formed Pt nanoparticles is higher in this solution, as aggregation to form a dense coagulum is a means to reduce the surface energy of the whole system. We are inclined to correlate the high surface energy of the newly formed Pt nanoparticles with the high energy barrier towards homogeneous nucleation in the solution containing SDS. This is in accordance with the experimental observation that SDS effectively depresses the homogeneous process such that Pt aggregation in solution was not observed (Figure 1A–C vs D).

When SDS was substituted by either *p*-$CH_3C_6H_4SO_3Na$ (sodium *p*-toluene sulfonate), $LiCF_3SO_3$ (lithium trifluoromethanesulfonate), or $LiClO_4$ (lithium perchlorate), TEM images revealed that selective depositions were achieved in all cases with little Pt aggregation in the solutions (Figure S4 in the Supporting Information). In the absence of CNTs, platinum coagulum was found to form in all of these solutions. These added salts share a common feature in that they all contain a weakly coordinating anion. As organic salts work equally as well as inorganic salts ($LiClO_4$), the role of the lipidic chain as a means to noncovalently modify CNTs[14] is downplayed, such that these salts are not expected to serve as a protecting or capping reagent. This is confirmed by EDS spectra, which show the absence of the elements of these salts in the as-prepared metal nanoparticles (Figure 2D). Polyvinylpyrrolidone (PVP) is a well-known protective reagent that aids metal particle dispersion in solution and prevents metal particles from aggregating through coordination effects.[13] When PVP was used, TEM images showed that selective deposition was unsuccessful (Figure 3). A large amount of Pt formed aggregates in solution, with only a small portion of the Pt being deposited on CNTs.

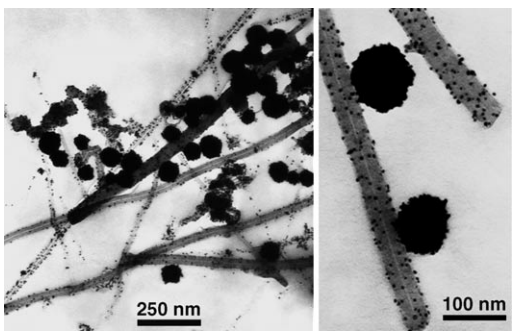

Figure 3. TEM images of Pt-coated MWNTs prepared by the addition of PVP.

There are few reports on the use of the addition of salts to direct selective metal deposition on the supports,[15] and the mechanism involved is unknown. However, the means by which salt addition facilitates colloidal aggregation is well understood.[16a] This salt effect is explained as follows. The counterions of the salt decrease the thickness of the electrical double layer (EDL) around each particle, thereby allowing the colloidal particles to come closer together. This in turn increases the van der Waals attraction and thus leads to a more rapid aggregation. The factors affecting the aggregation of transition-metal (TM) nanoparticles in solution have recently been studied systematically.[16a] It was shown that the EDL of TM nanoparticles in solution consists mainly of surface-adsorbed anions.[16a] Salt effects, as observed for colloids, can thus offer an explanation as to why salts such as SDS facilitate the formation of compact metal nanoparticles in our experiments (Figure 2B).

The formation of TM colloids or nanoparticles may involve three steps, namely nucleation, growth and aggregation.[16] It is generally accepted that the whole process is nucleation controlled. In other words, once the nucleus attains a critical size, TM clusters start to form at appreciable rates through autocatalytic growth.[16] For the initial nucleation of metal nanoparticles, there exist two possible mechanisms.[16–18] One mechanism assumes that the metal precursors first react with the reducing agents to give isolated TM^0 atoms, which then aggregate once a critical concentration is reached.[16a,17] The other supposes that a metallorganic precursor binds to another precursor to form an M–M bond. The addition of further precursors results in a growing cluster. Finally the cluster as a whole is reduced to the metallic state.[18] We extend these proposed mechanisms further and infer that the addition of salts to the solution would affect the nucleation barrier either by changing the free energy needed to create a solid/liquid interface or as a result of the adsorption of ions onto the newly formed TM^0 atoms.

Although the wetting of CNTs with metals is known to be generally poor,[12] the strengths of interaction of the CNT surface with metal atoms and metal clusters can differ significantly.[19] Recent QM calculations support the idea that TM^0 atoms bind sufficiently strongly (>2 eV for TM with open-shell d orbitals) to CNTs,[19a] while binding strengths decrease upon the formation of metal–metal bonds in the cluster.[19b] The bonds between the freshly formed Pt monomers and the CNT surfaces are expected to be strong. In fact, no Pt nanoparticles were observed to peel off into the solutions. The strong Pt–CNT bonds should promote heterogeneous nucleation, and disfavor the mechanism of homogeneous nucleation followed by deposition on CNTs.

We conclude that the mechanism for the selective deposition of Pt on CNTs by our method is as follows (Figure 4). Salt effects increase the barrier towards homogeneous nucleation, such that heterogeneous nucleation becomes more favorable. Once the critical nucleus size is attained, autocatalytic growth of the particle rapidly depletes the Pt-monomer concentration in the solutions, thereby effectively depressing homogeneous nucleation.

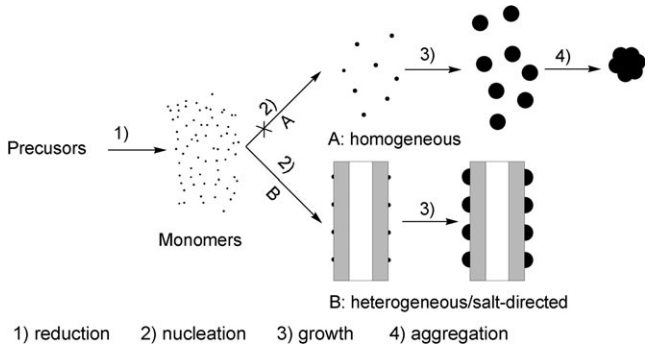

Figure 4. Schematic representation of salt-directed selective metal nucleation and growth on CNTs.

Size control of the deposited Pt nanoparticles: Although the Oswald ripening mechanism is well known for Ag-nanoparticle growth in solution, this mechanism is generally not applicable to Pt-nanoparticle growth.[13b,20] For Pt, it is believed that nanocrystal size control can only be realized by balancing the rates of nucleation and of growth from the monomers.[13b,20] Generally, a faster nucleation leads to more particles of smaller size, while a slower nucleation gives fewer particles of larger size.[13b,20] Several approaches have been developed for the synthesis of size-controlled Pt colloids by the reduction of Pt salts in aqueous or organic solution. Most of these approaches involve the use of stabilizing reagents (e.g., PVP or NaOH), which prevent the colloids from aggregating into larger particles.[10b,13,21,22] Particle size is controlled by changing the ratio of the amount of stabilizing reagent to the amount of Pt precursor,[13,21,22] the nature and/or the concentration of the reducing agent in solution,[13b] the mode of heating in the one-step reaction,[22] or by the combination of a one-step reaction with a stepwise-growth reaction (seed-mediated growth).[13b]

The method presented here is applicable to the size control of the deposited metal nanoparticles. No stabilizing reagents, such as PVP, are required in our method. Instead, we used salts such as SDS (2%). Size control of the particles was achieved by changing the concentration of metal ions (Figure 5B,C), the reaction temperature (Figure 5A–D), the reducing agent (Figure 5A) or the manner in which the solutions were added (Figure 5D). TEM images and the corresponding histograms given in Figures 5 and 6 demonstrate the size control of the Pt nanoparticles on SWNTs with 50% loading. Table 1 summarizes the mean diameters and the standard deviations (σ) of the sizes of the Pt nanoparticles.

The choice of reducing agent plays an important role in controlling the particle size. In general, a stronger reducing agent increases the rate of reduction of the metal ions, leading to smaller metal nanoparticles. When $NaBH_4$, a reducing agent stronger than EG, was used, a faster reduction rate tended to produce more Pt nuclei in a shorter period. This, in turn, hindered the growth of Pt nanoparticles, leading to CNTs coated with smaller particles. The histogram shown in Figure 6A indicates a mean metal-nanoparticle size of

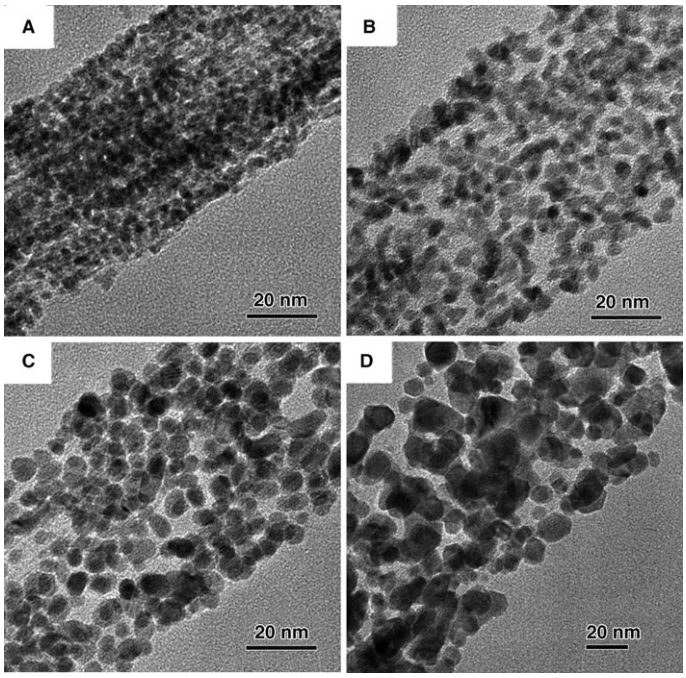

Figure 5. A)–D) TEM images, showing size control of the metal nanoparticles on CNTs (Pt-coated SWNTs, 50 wt%). See text for details. The corresponding HRTEM images are presented in Figure S6 in the Supporting Information.

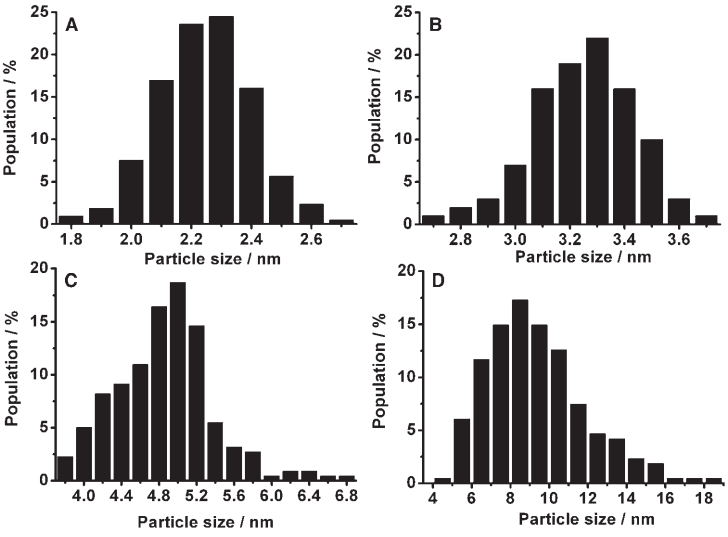

Figure 6. A)–D) Size distribution histograms of the Pt-coated SWNTs shown in Figure 5A–D, respectively.

Table 1. Mean particle sizes of the samples shown in Figure 5A–D.

	TEM size [nm]		XRD size [nm]
	Average diameter	Standard deviation	
A	2.3	0.29	2.1
B	3.3	0.35	3.1
C	4.9	1.02	4.7
D	9.6	4.26	9.1

2.3 nm, with a narrow size distribution ($\sigma = 0.29$ nm) and hence quite a uniform particle size. Here the synthesis was conducted as follows: CNTs (5 mg) were dispersed in a solution of H_2PtCl_6 (0.25 mg mL^{-1}) and SDS (2%) in EG (20 mL) at 100°C, into which a solution of $NaBH_4$ (5 mg mL^{-1}) in EG (1 mL; 5 mg mL^{-1}) was added dropwise.

Figures 5B,C show the change in the size of Pt nanoparticles as a function of an increase in the concentration of metal ions at constant temperature. For Figure 5B, a suspension of CNTs (2.5 mg) in a solution of H_2PtCl_6 (0.125 mg mL^{-1}) and SDS (2%) in EG (20 mL) was heated to 150°C, while for Figure 5C, a suspension of CNTs (10 mg) in a solution of H_2PtCl_6 (0.5 mg mL^{-1}) and SDS (2%) in EG (20 mL) was used. As the concentration of Pt ions was increased, the mean particle size increased from 3.3 nm (Figure 6B) to 4.9 nm (Figure 6C). At the same time, the size distribution broadened ($\sigma = 0.35$ and 1.02 nm, respectively). These results imply that increasing the concentration of the Pt precursors would decrease the number of the Pt nuclei, leading to Pt nanoparticles of larger size.

Figure 5D shows the Pt nanoparticles of larger size, produced by the seed-mediated growth approach. A suspension of CNTs (5 mg) in a solution of H_2PtCl_6 (0.0125 mg mL^{-1}) and SDS (2%) in EG (20 mL) was heated to 200°C. Pt seeds formed during this step. The system was subsequently cooled to 155°C, and a solution of H_2PtCl_6 (1 mg mL^{-1}) and SDS (2%) in EG (4.75 mL) was added dropwise over a period of 1.5 h. We observed that the Pt seeds that had already formed guided the subsequent Pt growth, leading to CNTs coated with larger Pt nanoparticles, with a mean diameter of 9.6 nm. The supported Pt nanoparticles, synthesized by this stepwise approach, were much larger than those produced by the one-step reaction (Figure 6D vs A–C), and the size distribution broadened further ($\sigma =$ 4.26 nm). This broader size distribution could be due to further nucleation in the second step of the Pt-nanoparticle growth stage.[24]

Temperature is an important factor for both selective nucleation and size control. For example, selective deposition of Pt nanoparticles on CNTs in EG with a Pt-ion concentration of 1 mg mL^{-1} was successful in the temperature range between 138°C and 160°C (c.f. Figure 5C). When the reaction temperature was raised to 180°C, aggregation of Pt nanoparticles in solution occurred. In the case of the stepwise-growth reaction, as shown in Figure 5D, temperatures as high as 200°C were required in order for seeds to form, due to the low concentration of Pt ions (0.0125 mg mL^{-1}). On the other hand, a lower temperature (155°C) was necessary in order to depress further nucleation during the growth stage. Thus the choice of an appropriate temperature is important for the balance of both heterogeneous/homogeneous nucleation and nucleation/growth processes.

The XRD patterns for the Pt-coated SWNTs shown in Figure 5A–D are shown in Figure 7. The diffraction peaks in each XRD pattern at 39.8, 46.2, 67.5, 81.3, and 85.8° can be assigned to reflections from the (111), (200), (220), (311), and (222) planes of the face-centered-cubic (fcc) Pt, and the

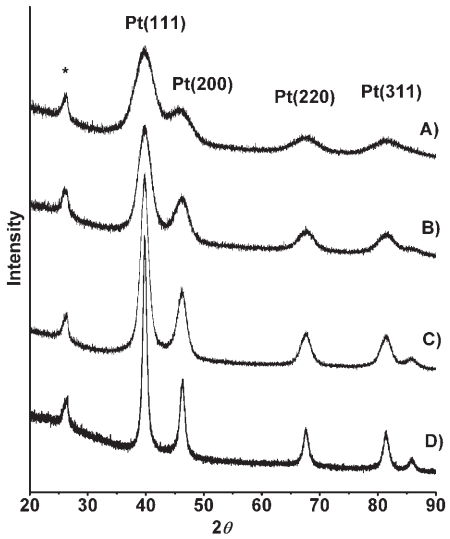

Figure 7. XRD patterns of the Pt-coated SWNTs shown in Figure 5A–D. A–D) correspond to metal nanoparticle sizes of 2.1, 3.1, 4.7 and 9.1 nm, respectively. The mean size of Pt particles was calculated from the Pt (220) XRD peak according to Scherrer's formula.[23] The peak labeled * is assigned to graphite.

diffraction peak at 26.5° can be assigned to a reflection from the (002) plane of graphite (SWNTs). The bandwidths of the Pt peaks in the diffractograms become narrower on going from A) to D), indicating an increase in the particle size. Table 1 summarizes the mean diameters of Pt nanoparticles, calculated from the XRD peak of the (220) reflection according to Scherrer's formula.[23] The particle sizes obtained from XRD are in close agreement with those determined from TEM, indicating a good crystallinity and dispersion of the supported Pt nanoparticles.[20]

Conclusion

We have presented a simple and versatile method for the synthesis of metal-coated carbon nanotubes by the reduction of metal ions in solution. We have performed controlled experiments to explore the underlying mechanisms, and have found that salt effects, well known in colloid chemistry, can be used to understand the observed facts in our experiments. Under the action of salt effects, our method effectively depresses homogeneous nucleation, leading to selective heterogeneous metal nucleation and growth on CNTs. Our method works well on CNTs both with and without preoxidation. We have shown that size control of metal nanoparticles can be achieved by changing the concentration of metal ions, the reaction temperature, the reducing agent or the means of adding solutions of reagents. Our method opens a door towards an understanding of the underlying mechanism of formation of a range of metal-coated CNTs. In addition, it may pave the way for the creation of novel hybrid materials with potential applications in many fields.

Experimental Section

Nanotube processing: The SWNTs and MWNTs used in this work were synthesized by a hydrogen-arc-discharge method[25a–b] and catalytic decomposition of hydrocarbons on an Fe catalyst, respectively.[25c–d] The pristine SWNTs were first purified and then preoxidized and cut by using a mixture of H_2SO_4 and HNO_3. MWNTs were prepurified with HCl, with no preoxidation. Details of the synthesis and pretreatment of the CNTs are provided in the Supporting Information (S1 and S2).

Preparation of Pt-coated CNTs: We used chloroplatinic acid (H_2PtCl_6) as the platinum precursor, and ethylene glycol as the solvent and reducing agent. We added sodium dodecyl sulfate (SDS) to the reaction system. In a typical synthesis, CNTs (5 mg) were mixed with a solution of SDS (2%) in EG (18 mL). After ultrasonication of the mixture for 1 h, a solution of H_2PtCl_6 (2.5 mg mL^{-1}) in EG (2 mL) was added under constant agitation. The reactive mixture was then heated in a 140 °C oil bath, and aged for 30 min under vigorous agitation to ensure completion of the reaction. The products were centrifuged, rinsed several times with ethanol and dried for future use. The Pt loading (given by the ratio: Pt/CNTs) of the products thus prepared was nominally 50 wt%. ICP-AES (inductively coupled plasma atomic-emission spectrometry) measurements yielded a metal loading of 47.7%.

The size control of platinum nanoparticles was realized by changing the concentration of the metal ions, the reaction temperature, the reducing agent, or the means by which the reactive solutions were added (see the Results and Discussion Section for details).

Instrumentation/techniques: The percentage loading of Pt on CNTs was verified by ICP-AES on an IRIS Intrepid II XSP ICP-AES instrument. The morphology of the products was investigated by the use of TEM, HRTEM, and scanning electron microscopy (SEM). Samples were ultrasonicated in ethanol and deposited onto holey carbon-coated copper grids. The TEM and HRTEM images were recorded on a JEM-100CXII or Hitachi-600 microscope operating at 100 kV and on a Tecnai F30 microscope, operating at 300 kV, respectively. The SEM images were recorded on a FESEM LEO 1530 instrument. Elemental analysis was performed with an X-ray energy-dispersive spectroscope attached to the Tecnai F30 TEM or LEO 1530 SEM. XRD analyses were carried out by using a PANalytical X'Pert powder X-ray diffractometer. XPS was performed on a PHI Quantum 2000 Scanning ESCA Microprobe (Physical Electronics) using Al-monochromatic X-ray at a power of 25 W with an X-ray-beam diameter of 100 μm, and a pass energy of 29.35 eV. The pressure of the analyzer chamber was maintained below $1x10^{-7}$ Pa during the measurement. The binding energy was calibrated using the C 1 s photoelectron peak at 284.6 eV as the reference.

Acknowledgements

This work was supported by the National Natural Science Foundation of China (20021002, 20533030, 50571085), the Ministry of Science and Technology of China (2001CB610506), and TRAPOYT from the Ministry of Education of China. We thank Z. X. Xie, Y. Chen, Y. X. Jiang, and Z. B. Chen for their help with the experiments; and Y.L. Chow, J. S. Shao and J. L. Yang for comments on the manuscript.

[1] a) K. J. C. Van Bommel, A. Friggeri, S. Shinkai, *Angew. Chem.* **2003**, *115*, 1010–1030; *Angew. Chem. Int. Ed.* **2003**, *42*, 980–999; b) A. Bezryadin, C. N. Lau, M. Tinkham, *Nature* **2000**, *404*, 971–974; c) S. Hrapovic, Y. Liu, K. B. Male, J. H. T. Luong, *Anal. Chem.* **2004**, *76*, 1083–1088; d) J. M. Planeix, N. Coustel, B. Coq, V. Brotons, P. S. Kumbhar, R. Dutartre, P. Geneste, P. Bernier, P. M. Ajayan, *J. Am. Chem. Soc.* **1994**, *116*, 7935–7936; e) G. Che, B. B. Lakshmi, E. R. Fisher, C. R. Martin, *Nature* **1998**, *393*, 346–349; f) K. Y. Chan, J. Ding, J. Ren, S. Cheng, K. Y. Tsang, *J. Mater. Chem.* **2004**, *14*, 505–516.

[2] a) B. C. Satishkumar, E. M. Vogl, A. Govindaraj, C. N. R. Rao, *J. Phys. D* **1996**, *29*, 3173–3176; b) R. Q. Yu, L. W. Chen, Q. P. Liu, J. Y. Lin, K. L. Tan, S. C. Ng, H. S. O. Chan, G. Q. Xu, T. S. A. Hor, *Chem. Mater.* **1998**, *10*, 718–722; c) V. Lordi N. Yao, J. Wei, *Chem. Mater.* **2001**, *13*, 733–737; d) W. Z. Li, C. H. Liang, W. J. Zhou, J. S. Qiu, Z. H. Zhou, G. Q. Sun, Q. Xin, *J. Phys. Chem. B* **2003**, *107*, 6292–6299; e) R. Giordano, P. Serp, P. Kalck, Y. Kihn, J. Schreiber, C. Marhic, J. L. Duvail, *Eur. J. Inorg. Chem.* **2003**, 610–617; f) Y. C. Xing, *J. Phys. Chem. B* **2004**, *108*, 19255–19259; g) C.-H. Li, Z.-X. Yu, K.-F. Yao, S.-f. Ji, J. Liang, *J. Mol. Catal. A* **2005**, *226*, 101–105.

[3] S. Banerjee, S. S. Wong, *J. Am. Chem. Soc.* **2003**, *125*, 10342–10350.

[4] a) X. R. Ye, Y. H. Lin, C. M. Wai, *Chem. Commun.* **2003**, 642–643; b) X. R. Ye, Y. H. Lin, C. M. Wang, C. M. Wai, *Adv. Mater.* **2003**, *15*, 316–319; c) Z. Y. Sun, Z. M. Liu, B. X. Han, Y. Wang, J. M. Du, Z. L. Xie, G. J. Han, *Adv. Mater.* **2005**, *17*, 928–932.

[5] a) Q. Q. Li, S. S. Fan, W. Q. Han, C. H. Sun, W. S. Liang, *Jpn. J. Appl. Phys. Part 2* **1997**, *36*, L501–L503; b) L. M. Ang, T. S. A. Hor, G. Q. Xu, C. H. Tung, S. P. Zhao, J. L. S. Wang, *Carbon* **2000**, *38*, 363–372; c) Z. L. Liu, X. H. Lin, J. Y. Lee, W. Zhang, M. Han, L. M. Gan, *Langmuir* **2002**, *18*, 4054–4060; d) F. Wang, S. Arai, M. Endo, *Electrochem. Commun.* **2004**, *6*, 1042–1044.

[6] a) K. Y. Jiang, A. Eitan, L. S. Schadler, P. M. Ajayan, R. W. Siegel, N. Grobert, M. Mayne, M. Reyes-Reyes, H. Terrones, M. Terrones, *Nano Lett.* **2003**, *3*, 275–277; b) A. V. Ellis, K. Vjayamohanan, R. Goswaimi, N. Chakrapani, L. S. Ramanathan, P. M. Ajayan, G. Ramanath, *Nano Lett.* **2003**, *3*, 279–282; c) A. Carrillo, J. A. Swartz, J. M. Gamba, R. S. Kane, N. Chakrapani, B. Q. Wei, P. M. Ajayan, *Nano Lett.* **2003**, *3*, 1437–1440; d) L. Liu, T. X. Wang, J. X. Li, Z. X. Guo, L. M. Dai, D. Q. Zhang, D. B. Zhu, *Chem. Phys. Lett.* **2003**, *367*, 747–752; e) B. Kim, W. M. Sigmund, *Langmuir* **2004**, *20*, 8239–8242; f) L. Han, W. Wu, F. L. Kirk, J. Luo, M. M. Maye, N. N. Kariuki, Y. H. Lin, C. M. Wang, C. J. Zhong, *Langmuir* **2004**, *20*, 6019–6025; g) B. J. Taft, A. D. Lazareck, G. D. Withey, A. Yin, J. M. Xu, S. O. Kelley, *J. Am. Chem. Soc.* **2004**, *126*, 12750–12751; h) V. Georgakilas, V. Tzitzios, D. Gournis, D. Petridis, *Chem. Mater.* **2005**, *17*, 1613–1617; i) G. M. A. Rahman, D. M. Guldi, E. Zambon, L. Pasquato, N. Tagmatarchis, M. Prato, *Small* **2005**, *1*, 527–530; j) M. A. Correa-Duarte, J. Pérez-Juste, A. Sánchez-Iglesias, M. Giersig, L. M. Liz-Marzán, *Angew. Chem.* **2005**, *117*, 4449–4452; *Angew. Chem. Int. Ed.* **2005**, *44*, 4375–4378.

[7] a) Q. Xu, L. Zhang, J. Zhu, *J. Phys. Chem. B* **2003**, *107*, 8294–8296; b) H. Tang, J. H. Chen, S. Z. Yao, L. H. Nie, G. H. Deng, Y. M. Kuang, *Anal. Biochem.* **2004**, *331*, 89–97; c) S. Arai, M. Endo, N. Kaneko, *Carbon* **2004**, *42*, 641–644; d) D. J. Guo, H. L. Li, *Electrochem. Commun.* **2004**, *6*, 999–1003; e) G. Girishkumar, K. Vinodgopal, P. V. Kamat, *J. Phys. Chem. B* **2004**, *108*, 19960–19966; f) B. M. Quinn, C. Dekker, S. G. Lemay, *J. Am. Chem. Soc.* **2005**, *127*, 6146–6147; g) T. M. Day, P. R. Unwin, N. R. Wilson, J. V. Macpherson, *J. Am. Chem. Soc.* **2005**, *127*, 10639–10647.

[8] a) Y. Zhang, H. J. Dai, *Appl. Phys. Lett.* **2000**, *77*, 3015–3017; b) Y. Zhang, N. W. Franklin, R. J. Chen, H. J. Dai, *Chem. Phys. Lett.* **2000**, *331*, 35–41.

[9] a) S. H. Joo, S. J. Choi, I. Oh, J. Kwak, Z. Liu, O. Terasaki, R. Ryoo, *Nature* **2001**, *412*, 169–172; b) J. S. Yu, S. Kang, S. B. Yoon, G. Chai, *J. Am. Chem. Soc.* **2002**, *124*, 9382–9383; c) T. Hyeon, S. Han, Y. E. Sung, K. W. Park, Y. W. Kim, *Angew. Chem.* **2003**, *115*, 4488–4492; *Angew. Chem. Int. Ed.* **2003**, *42*, 4352–4356; d) M. Endo, Y. A. Kim, M. Ezaka, K. Osada, T. Yanagisawa, T. Hayashi, M. Terrones, M. S. Dresselhaus, *Nano Lett.* **2003**, *3*, 723–726.

[10] a) B. C. Gates, *Chem. Rev.* **1995**, *95*, 511–522; b) A. Roucoux, J. Schulz, H. Patin, *Chem. Rev.* **2002**, *102*, 3757–3778.

[11] a) M. Mertig, L. C. Ciacchi, R. Seidel, W. Pompe, A. De Vita, *Nano Lett.* **2002**, *2*, 841–844; b) J. Richter, *Phys. E* **2003**, *16*, 157–173; c) R. Seidel, L. C. Ciacchi, M. Weigel, W. Pompe, M. Mertig, *J. Phys. Chem. B* **2004**, *108*, 10801–10811.

[12] E. Dujardin, T. W. Ebbesen, H. Hiura, K. Tanigaki, *Science* **1994**, *265*, 1850–1852.

[13] a) R. Narayanan, M. A. El-Sayed, *J. Am. Chem. Soc.* **2003**, *125*, 8340–8347; b) T. Teranishi, M. Hosoe, T. Tanaka, M. Miyake, *J.*

Phys. Chem. B **1999**, *103*, 3818–3827; c) F. Bonet, V. Delmas, S. Grugeon, R. H. Urbina, P. Y. Silvert, K. Tekaia-Elhsissen, *Nano-Struct. Mater.* **1999**, *11*, 1277–1284.
[14] C. Richard, F. Balavoine, P. Schultz, T. W. Ebbesen, C. Mioskowski, *Science*, **2003**, *300*, 775–778.
[15] B. Liu, H. C. Zeng, *J. Phys. Chem. B* **2004**, *108*, 5867–5874.
[16] a) B. J. Hornstein, R. G. Finke, *Chem. Mater.* **2004**, *16*, 139–150; b) A. Cacciuto, S. Auer, D. Frenkel, *Nature* **2004**, *428*, 404–406; c) U. Gasser, E. R. Weeks, A. Schofield, P. N. Pusey, D. A. Weitz, *Science* **2001**, *292*, 258–262.
[17] D. G. Duff, P. P. Edwards, B. F. G. Johnson, *J. Phys. Chem.* **1995**, *99*, 15934–15944.
[18] a) L. C. Ciacchi, W. Pompe, A. De Vita, *J. Am. Chem. Soc.* **2001**, *123*, 7371–7380; b) J. Turkevich, P. C. Stevenson, J. A. Hillier, *Discuss. Faraday Soc.* **1951**, *11*, 55.
[19] a) E. Durgun, S. Dag, V. M. K. Bagci, O. Gulseren, T. Yildirim, S. Ciraci, *Phys. Rev. B* **2003**, *67*, 201401; b) A. Maiti, A. Ricca, *Chem. Phys. Lett.* **2004**, *395*, 7–11.
[20] E. V. Shevchenko, D. V. Talapin, H. Schnablegger, A. Kornowski, O. Festin, P. Svedlindh, M. Haase, H. Weller, *J. Am. Chem. Soc.* **2003**, *125*, 9090–9101.
[21] Y. Wang, J. W. Ren, K. Deng, L. L. Gui, Y. Q. Tang, *Chem. Mater.* **2000**, *12*, 1622–1627.
[22] W. Y. Yu, W. X. Tu, H. F. Liu, *Langmuir* **1999**, *15*, 6–9.
[23] V. Radmilovic, H. A. Gasteiger, P. N. Ross, *J. Catal.* **1995**, *154*, 98.
[24] R. Nikhil, N. R. Jana, L. Gearheart, C. J. Murphy, *Chem. Mater.* **2001**, *13*, 2313–2322.
[25] a) C. Liu, H. T. Cong, F. Li, P. H. Tan, H. M. Cheng, K. Lu, B. L. Zhou, *Carbon* **1999**, *37*, 1865–1868; b) C. Liu, Y. Y. Fan, M. Liu, H. T. Cong, H. M. Cheng, M. S. Dresselhaus, *Science* **1999**, *286*, 1127–1129; c) Y. Y. Fan, F. Li, H. M. Cheng, G. Su, Y. D. Yu, Z. H. Shen, *J. Mater. Res.* **1998**, *13*, 2342–2346; d) P. X. Hou, S. Bai, Q. H. Yang, C. Liu, H. M. Cheng, *Carbon* **2002**, *40*, 81–85.

Received: August 19, 2005
Published online: January 3, 2006

